



On the drivers of Mediterranean Marine Cold Spells under Climate Change

Sofia Darmaraki¹, Marco Reale², Robin Waldman³, Vassiliki Metheniti¹,

5 ¹Foundation for Research and Technology, Hellas (FORTH), Greece, Crete

²National Institute of Oceanography and Applied Geophysics-OGS, Trieste, Italy

³Météo-France, CNRS, Univ. Toulouse, CNRM, Toulouse, France

Correspondence to: Sofia Darmaraki (sofia.darm@gmail.com)

10

15

20



Abstract. Marine Cold Spells (MCSs) are prolonged, extreme cold temperature events in the ocean that can disturb marine ecosystems. Here, we analyze for the first time historical (1980–2014) and future (2015–2100) MCSs in the Mediterranean Sea, using the output from a high-resolution regional climate system model, under global warming levels 1–4°C and the high-emission climate change scenario SSP5-8.5. Historically, atmosphere forcing dominates open-ocean MCSs in all seasons, except winter, where Advection plays a more dominant role across the basin, reflecting the influence of alongshore currents and mesoscale variability in dynamically active regions. Mixing drives coastal and localized events mostly in the summer, likely due to regional wind forcing. As global temperatures rise, projections relative to a fixed historical baseline indicate up to 92% decline in future MCS occurrence, up to a 50% reduction in their duration and up to 19% decrease in their intensity already by 2036-2055. These changes are more pronounced during winter, with the events becoming increasingly confined to the northern Mediterranean and progressively disappearing. When defined relative to a shifted climatology, future MCSs represent extreme cold events of a warmer climate and are projected to become less frequent, slightly longer and more intense compared to the past by the end of the century. The driving mechanisms of both types of future MCSs shift from a dominant atmospheric control in the historical period towards an increasing influence of oceanic advection and mixing, particularly in the summer, autumn and spring and by the end of the century.

1. Introduction

Marine Cold Spells (MCSs) are defined as a continuous period of extreme cold temperature events affecting the surface or the entire water column in the coastal or open ocean, where they can drive abrupt and significant changes in marine biodiversity and ecosystem functioning (Schlegel et al., 2021). Over the last decades, there has been a dramatic decrease in MCS frequency, duration and intensity in certain regions of the global ocean (Schlegel et al., 2017), including the Mediterranean Sea (Simon et al., 2022; Ciappa, 2022). Although MCS trends and spatial distribution are not well studied in the basin, Simon et al. (2022) revealed a higher occurrence of MCS in the western Mediterranean (WMED) between 1982-2021, while the Eastern Mediterranean (EMED) featured a more profound MCS decline, potentially linked to the warming of the area (Kotta et Kitsiou, 2019), despite experiencing some of the strongest MCSs ever recorded in the region (winter 1983, 1984 and 1992).

To date, most documented Mediterranean MCSs have been associated with dense water formation events (DWF). For example, one of the most severe MCSs occurred in the Adriatic Sea during the winter of 2012, where seawater temperatures reached values as low as 4°C, due to strong and persistent northeasterly winds and large surface heat losses to the atmosphere. The exceptionally cold and dense water masses that were formed spread quickly throughout the deepest parts of the basin (Mihanović et al., 2013; Raicich et al., 2013; Chiggiato et al., 2016a,b; Querin et al., 2016), altering deep stratification (Bensi et al., 2013). In some coastal locations of eastern Adriatic this event was preconditioned by a reduction in the typical freshwater input, following an unusually dry and warm preceding year (Mihanović et al., 2013; Janeković et al.,



55 2014). The exceptionally cold and windy conditions that ultimately triggered the MCS were attributed to an interplay
between deep lows (Chiggiato et al., 2016b) developing over the Mediterranean Sea (Raicich et al., 2013), particularly
affecting the central and south Adriatic Sea (Mihanović et al., 2013) and to a persistent and stable anticyclonic atmospheric
circulation that extended over central Europe. Such an intense atmosphere blocking scenario manifests rarely over the
Adriatic Sea (Mihanović et al., 2013), with the last notable occurrences documented in 1929 and 1956 (Penzar et al., 2001).
60 The 2012 MSC ended due to a sudden drop in windspeed. Similarly cold, windy and anomalously dry winters triggered
major DWF events in the WMED during 2005 (López-Jurado et al., 2005; Salat et al., 2006; Font et al., 2007; Schroeder et
al., 2008; Guillén et al., 2018), in the Aegean Sea during the winter of 2016/2017 (Velaoras et al., 2017) and in the Cretan
Sea in 2022 (Teruzzi et al., 2024).

A notable MCS occurred in October 2021, during interactions between Medicane Apollo and the permanent cyclonic gyre
65 in the western Ionian Sea. The dramatic drop in the temperature of the cyclonic gyre core was attributed to increased wind-
stress curl, Ekman pumping and relative vorticity. Unlike previous atmospheric cyclones, surface layers in the cyclonic gyre
area cooled as vertical mixing was combined with upwelling in the subsurface layers, leading to shoaling of mixed layer
depth (MLD), nutricline and halocline (Menna et al., 2023).

MCS have been observed to enhance productivity in the ocean surface (Auger et al. 2014; Terruzzi et al., 2024), but their
70 impacts in the Mediterranean Sea vary. While anomalous DWF have caused fisheries collapse (Company et al., 2008; Martin
et al., 2016) they have also enhanced trophic webs of deep-sea, sessile benthic communities (Orejas et al., 2009; Gori et al.,
2013; Taviani et al., 2016). The intense and prolonged cold outbreak that affected the Gulf of Trieste in February 2018 led to
a transient oligotrophy regime, changes in biogeochemistry of coastal systems and constrained the microbial processing of
organic matter, further hindering metabolic recovery following the event's conclusion (Manna et al., 2019). In 1991, a strong
75 cold-air outbreak over the shallow Thessaloniki Bay, combined with very cold water transport from nearby rivers, resulted in
a mass mortality event of approximately 794 tonnes of the fish species *Sardinella aurita Valenciennes*, due to thermal shock
(Economidis et Vogiatzis, 1992). Cold stress can also trigger acclimatory responses, as shown by increased metabolic rates in
Anomalocardia flexuosa during simulated winter cold spells (Carneiro et al., 2020).

Despite their significant impacts on the marine environment, the drivers of historical MCSs in the Mediterranean Sea
80 have not been systematically examined, with research largely focusing on their warm counterparts, marine heatwaves
(Darmaraki et al., 2024). Existing research on cold extremes in the basin has also largely focused on winter DWF processes,
with the mechanisms leading to MCS in other seasons remaining unexplored. Moreover, no study to date has investigated
how climate change may alter MCS characteristics and their underlying mechanisms.

Here, we address these gaps by providing for the first time, projections of future MCS characteristics and drivers in the
85 Mediterranean Sea. We use the output of a coupled regional climate system model developed for the Mediterranean Sea to
investigate local-scale MCS properties and related drivers across historical (1980-2014) and future (2015-2100) periods. We
assess projected changes of future MCS characteristics and their drivers under global warming scenarios 1°C, 2°C, 3°C and
4°C above the pre-industrial era, under the high-emission scenario SSP5-8.5. The paper is organised as follows: Section 2



presents the datasets and methodologies used to identify MCS. The results of our analysis are discussed in Section 3, with the conclusions provided in Section 4.

2. Methods

2.1 Datasets

To investigate the past and future characteristics and drivers of Mediterranean MCSs, we use the outputs from the high-resolution (6–8 km), fully coupled regional climate system model CNRM-RCSM6 (Sevault, 2024; Darmaraki et al., 2019b) from the Med-CORDEX-CMIP6 initiative (Ruti et al., 2016; Somot et al., 2018). The modeling system includes the ocean model NEMOMED12 (Beuvier et al., 2012; Madec et al., 2022), with a horizontal resolution of $1/12^\circ$ and 75 uneven vertical levels (including 7 in the upper 10 m) and covers the entire Mediterranean Sea. We analyze daily sea surface temperature (SST), mixed layer temperature (MLT), mixed layer depth (MLD) and both atmospheric and oceanic heat flux components. The model's historical and scenario runs have already been extensively used to assess past and future changes in Mediterranean surface circulation and sea level (Parras-Berrocal et al., 2024; 2025), as well as surface and subsurface marine heatwaves (Darmaraki et al., 2019a; 2025 in review).

To identify historical and future MCS in this work we apply the Hobday et al. (2016) definition on daily MLT. Prior to this analysis we assess the model's skill in reproducing historical MCSs in the Mediterranean Sea, by applying the MCS detection framework on the modeled SST, due to the lack of observational datasets with sufficient spatial and temporal coverage of MLT. In particular, the surface MCSs identified from the model are compared against observed events identified from the reprocessed Mediterranean Sea, high resolution Level-4 SST product (https://data.marine.copernicus.eu/product/SST_MED_SST_L4_REP_OBSERVATIONS_010_021/description, Pisano et al., 2016). This dataset provides daily, satellite-derived SST at 0.05° resolution for the period 1982–2017. The differences between the events identified from the model's SST and MLT are elaborated in the discussion section.

The CNRM-RCSM6 hindcast simulation between 1982–2017 is used as an additional reference simulation against which historical surface MCS characteristics are compared. This hindcast simulation has previously been validated in Darmaraki et al., (2019b), in addition to the skill of the model in reproducing the seasonal mean SST features in Darmaraki et al. (2025, *in review*)

2.2 MCS detection

As introduced in the previous section, we identify MCSs using the detection framework of Hobday et al. (2016), but we apply here the updated version by Petrelli, (2022) (<https://github.com/coecms/xmhw>). According to this approach a MCS is found when the daily SST falls below the seasonally varying 10th percentile threshold, relative to a 30-year baseline, for at least 5 consecutive days. Detection is applied daily at each grid point, producing gridded fields of MCS presence/absence. Each event is separated into onset (start to peak) and decay (peak to end) phases and is further categorized into seasons based



120 on the date of its onset (e.g., an event beginning in autumn but ending in winter is classified as an autumn MCS). This approach allows us to identify seasonal frequency, mean duration and intensity (mean temperature anomaly throughout the event's duration relative to climatology) of each MCS in addition to their seasonal drivers throughout their development phase.

125 First, we compare surface MCS properties identified in the CNRM-RCSM6 historical run with those detected from the satellite dataset and the output from the CNRM-RCSM6 hindcast run. By using a common 1982–2014 climatological baseline, we ensure consistent thresholds and comparability between observed and simulated MCSs. However, as MLT better reflects heat content variations within the mixed layer, characteristics and underlying mechanisms of MCSs are subsequently assessed using MLT in both the historical and SSP5-8.5 runs.

130 The characteristics and drivers of the historical MCSs are compared with those of future MCSs under global warming levels (GWLs) +1°C, +2°C, +3°C and +4°C relative to the pre-industrial period of (1850–1900). The future GWL periods are determined based on the years when the driving global climate model of the RCSM (CNRM-ESM2-1) reaches each respective GWL, following the methodology applied in CMIP5 and CMIP6 by Hauser et al. (2022) (see Table S1). This framework has previously been adopted for Mediterranean climate projections by Parras-Berrocal et al. (2024). Finally, following the methodology applied for MHWs by Darmaraki et al. (2025, in review), future MCSs are identified using two approaches: (a) a fixed 1982–2014 baseline and (b) shifting climatology centered on each of the GWL1–GWL4 (see Table S1). This approach allows us to examine future MCSs under two climate states: one that preserves the long-term climate change signal (fixed baseline) and another that removes it by accounting for the evolving mean state (shifting baseline).

2.3 Mixed Layer Heat Budget Analysis of MCS Drivers

140 To identify the drivers of MCSs, we use a daily mixed layer heat budget (MLHB) analysis, which links daily MLT variations with changes in heat contributions from atmospheric forcing, oceanic advection and mixing processes. The MLHB (Caniaux et al., 1998) is expressed as:

$$\underbrace{\frac{\partial \bar{T}}{\partial t}}_{\text{A) MLT Tendency}} = \underbrace{\frac{Q_{SW} + Q_{LW} + Q_{sens} + Q_{Lat} - Q_{SW}|_{-h}}{\rho_0 C_p h}}_{\text{B) Forcing}} - \underbrace{\nabla \cdot (\mathbf{uT})}_{\text{C) Advection}} - \underbrace{\frac{(\bar{T} - T_{-h}) \frac{\partial h}{\partial t}}{h} + \nabla_H \cdot (\mathbf{K}_H \nabla_H \mathbf{T}) - \frac{(K_z \frac{\partial T}{\partial z})|_{-h}}{h}}_{\text{D) Mixing}} \quad (\text{Eq.1})$$

145 , where $\bar{T} = \frac{1}{h} \int_{-h}^0 T dz$ is the average of MLT over MLD thickness h and t is time in days. Q_{SW} , Q_{LW} , Q_{sens} , Q_{Lat} are shortwave, longwave, sensible and latent heat fluxes, $\rho_0=1035 \text{ kg m}^{-3}$ the seawater density, $C_p=3992 \text{ J kg}^{-1} \text{ }^\circ\text{C}$ the ocean heat capacity, $\mathbf{u} = (u,v,w)$ the velocity vector, ∇_h the horizontal gradient and K_H, K_z are the horizontal and vertical diffusion coefficients. The MLD is time-varying, defined by $\Delta\rho = 0.01 \text{ kg m}^{-3}$ and a minimum depth of 10 m (Tréguier et al., 2023).



Processes are grouped into: Forcing (net atmospheric heat fluxes), Advection (horizontal and vertical transport) and Mixing, which encompasses local entrainment/detrainment and turbulent transports, dominated by vertical mixing. All terms are explicitly computed, except from local entrainment/detrainment which is deduced as a residual of the budget over the time-varying mixed layer depth. The budget is vertically averaged at each grid point and time step.

The total anomalous change in mixed-layer heat content during the MCS onset period is quantified at each grid point, by the corresponding cumulative anomalies of daily MLT (Term A, Eq. 1) relative to the climatological period. The local dominant MCS driver is then identified as the process removing the highest, cumulative heat content (highest anomalous negative heat contribution) throughout the onset period, relative to the corresponding, total anomalous change in MLT. Each anomalous MLHB contribution is described below at each location as:

$$C_p = \frac{\int_{t_1}^{t_2} H_{anom}^p(t) dt}{\int_{t_1}^{t_2} \frac{dT_{anom}(t)}{dt} dt} \quad (\text{Eq.2})$$

, where C_p is the dimensionless fractional contribution of a process p , H_{anom}^p the daily anomalous heat contribution relative to the respective climatology ($^{\circ}\text{C}/\text{day}$) of a process p , $\overline{T_{anom}}(t)$ the daily anomalous MLT tendency ($^{\circ}\text{C}/\text{day}$) and t_1, t_2 the starting and peak dates of a given MCS onset. A negative anomaly of atmospheric forcing reflects enhanced net surface heat losses and a negative anomaly of advection indicates anomalous import of colder waters. For vertical mixing, a negative value typically represents enhanced entrainment of colder subsurface water, reinforcing cooling, whereas a positive value implies reduced cold entrainment or mixing which acts to damp the MCS.

To investigate how MCSs change in response to climate change, we first construct maps showing the fraction of historical MCSs primarily driven by Forcing (f_{for}), Advection (f_{adv}) and Mixing (f_{mix}) relative to the total number of events at each location, for each season and period. We then assess changes in the frequency of MCSs associated with each driving process between the future and historical periods across seasons, expressed as percentage changes at each location:

$$\Delta f_{(i,j)}^p = f_{(i,j)future}^p - f_{(i,j)hist}^p \quad (\text{Eq.3})$$

, where $f_{(i,j)hist}^p = \frac{N_{hist}^p}{N_{tot}^{hist}} \%$ and $f_{(i,j)future}^p = \frac{N_{future}^p}{N_{tot}^{future}} \%$ with $p \in \{for, adv, mix\}$, N^p the number of MCSs primarily driven by a given process p in a specific location (i,j) and N^{tot} the total number of MCSs in a given period and that location.

3.Results and Discussion:

3.1 Model Evaluation

The model's ability to simulate past MCSs is evaluated by comparing the seasonal mean characteristics of the observed and simulated surface events. To ensure a consistent comparison, the satellite data were interpolated to the model grid at a



horizontal resolution of $1/12^\circ$. Throughout the period 1982-2014, the hindcast and historical runs tend to slightly
 180 overestimate (14-18 events; Table S2) the observed basin-mean number of MCS across seasons (11-14 events, Table S2).
 Nevertheless, both runs capture the spring maximum in the basin-mean MCS number (Fig. 1b,f,j), with the historical
 simulation suggesting a comparably high MCS number in the summer (Fig. 1k). The northwestern Mediterranean, Adriatic
 and Aegean Sea are identified as MCS hotspots in the observations and both simulations, while the southern Mediterranean
 Sea shows lower MCS counts across all seasons but winter. That season displays the lowest basin-mean MCS count in both
 185 simulations and particularly in the Ionian Sea and the Levantine Basin (Fig. 1e,i). The observed MCS count was found
 similarly low in winter, with only one more event identified than the summer minimum.

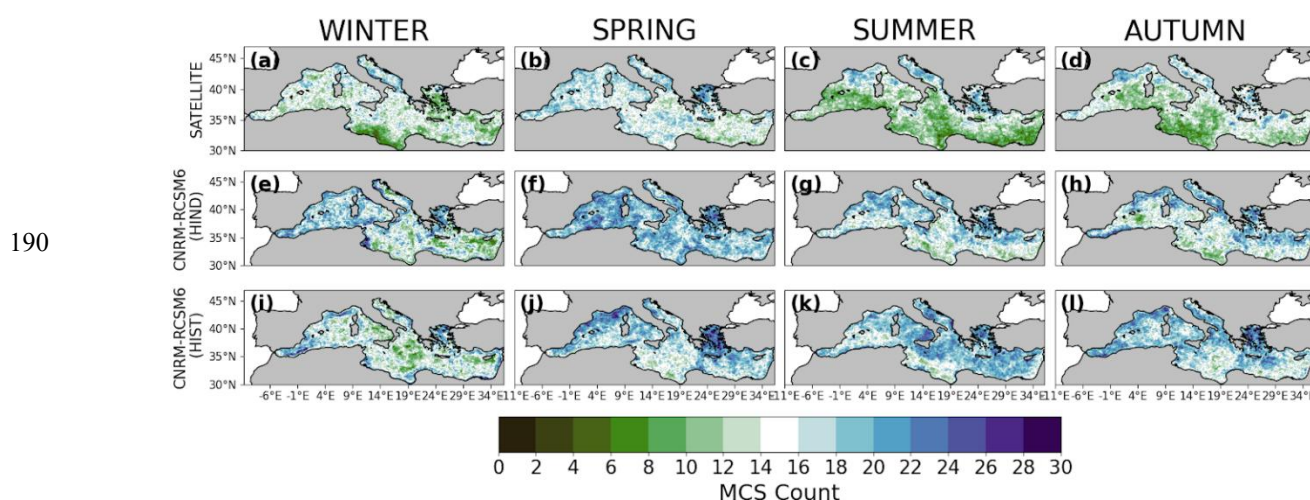


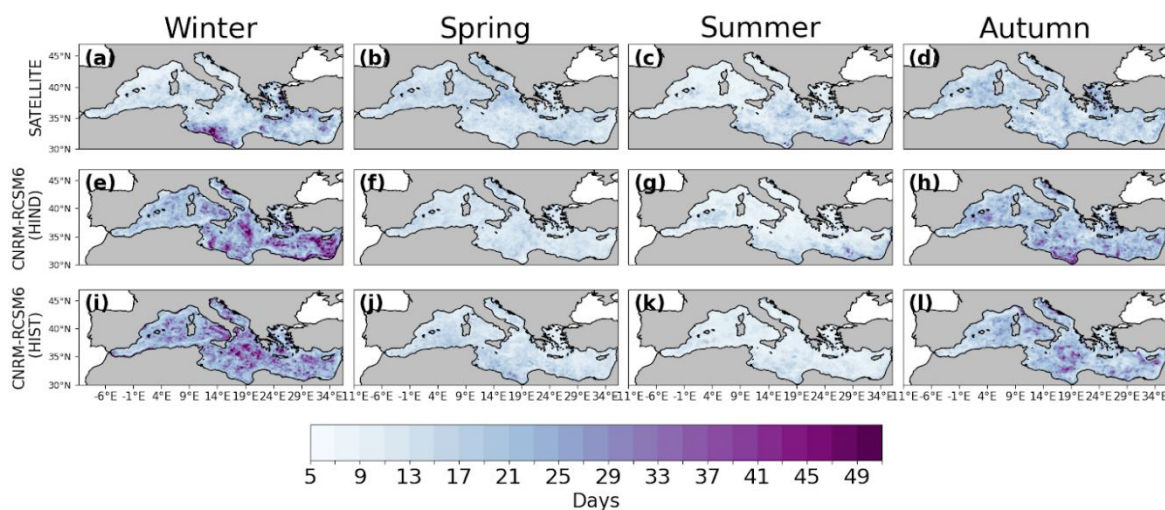
Figure 1: Total number of historical surface MCSs in the Mediterranean Sea across seasons throughout 1982-2014. The
 number of events is shown locally for winter (DJF), spring (MAM), summer (JJA) and autumn (SON). Row corresponds to
 195 events detected in a-d) satellite dataset, e-h) CNRM-RCSM6 hindcast, and i-l) CNRM-RCSM6 historical simulations. MCSs
 were identified by applying Hobday et al. (2016) to SST, with 1982–2014 as the baseline climatology. Seasons are assigned
 based on the MCS onset date, regardless of termination.

The regions and seasons with low MCS count tend to display a more persistent behaviour. Specifically, MCSs in winter
 (14–21 days) and autumn (14–18 days) are longer, on average, than MCSs in spring (12–13 days) and summer (10–11 days)
 200 across all datasets (Table S2). While in spring and summer the datasets show no significant differences in their basin-mean
 duration (Fig. 2b,c,f,g,j,k Table S2), the corresponding pattern correlation coefficients (-0.05 to 0.4) indicate limited spatial
 agreement with the observations ($3 < \text{RMSE} < 6.9$ days, Table S3). In winter, the historical basin-mean MCS duration is
 higher than the duration of both the observations and the hindcast run (Fig. 2a,e,i), while in autumn it is higher than the
 observed values but lower than the hindcast run (Fig. 2d,h,l). The discrepancies are more pronounced in winter
 205 ($8 < \text{RMSE} < 11$, $\text{corr. coeff} < 0.3$, Table S3) and particularly over the Central Mediterranean Sea (CMED, Table S3), in parts of

the Levantine basin and the Tyrrhenian Sea, where simulated local MCS persist for 50–90 days, in contrast to ~5–30 days in the observations and ~60 days in the hindcast simulation.

210 These results indicate that although the historical simulation slightly overestimates the observed basin-mean surface MCS number and duration it captures their observed seasonal variability, with fewer and longer MCSs in winter and autumn and more frequent and shorter events in spring and summer. However, the low Pearson correlation coefficients and moderate RMSEs imply that the historical simulation does not capture efficiently the spatial distribution of MCS count and duration. This bias likely reflects differences between near-surface (0.5 m) model temperatures and satellite skin-layer measurements and reduced short-term variability in modeled SST compared to observations (e.g. Pilo et al., 2019). A similar effect may also influence the observed MCSs characteristics, as the satellite data were interpolated prior to analysis.

215



225

Figure 2: As in Figure 1 but for average surface MCS duration throughout the period 1982-2014.

Both runs are also consistent with the observations in simulating higher basin-mean surface MCS intensity in summer (-2 °C) and autumn (-1.6 to -1.8 °C) relative to winter (-1.3 to -1 °C) and spring (-1.5 to -1.7 °C) (Table S2). While the historical simulation tends to underestimate the observed basin-mean MCS intensity across all seasons (RMSE ≈ 0.3 °C; correlation coefficient: 0.3–0.7, Table S4,S2), its magnitude and spatial patterns are comparable to, or slightly stronger than, those of the surface MCS identified in the hindcast run (RMSE 0.2–0.3 °C; correlation coefficient 0.7–0.9, Table S4). Both runs capture in summer and autumn the observed north–south gradient in surface MCS intensity, with strongest anomalies in the northern Mediterranean and particularly the Gulf of Lions (~ -4.5°C) and weakest values (~ -1.5 °C) in the south (Fig. 3c,d,g,h,k,l). In winter (Fig. 3a,e,i) and spring (Fig. 3b,f,j), however, surface MCS intensities are more uniformly distributed across the basin. Overall, the historical run underestimates slightly the observed basin-mean intensity of surface MCSs but it qualitatively captures their seasonal variability, with more intense events in summer and less intense in winter. The spatial patterns of observed MCS intensity are reproduced by both the historical and hindcast run.

235



240

245

250

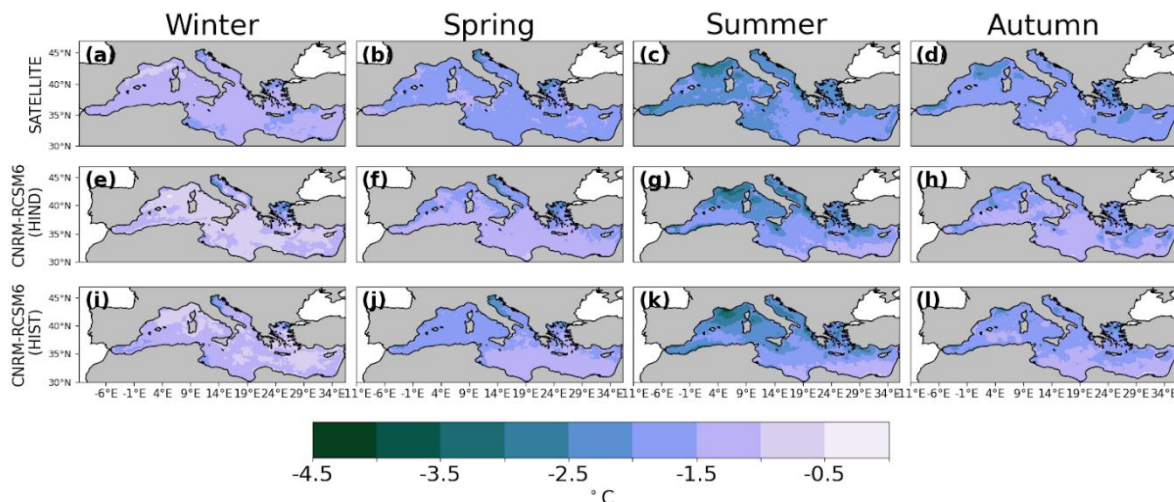


Figure 3: As in Figure 1 but for mean MCS intensity throughout the period 1982-2014.

The characteristics of the historical surface MCSs are physically consistent with Mediterranean upper-ocean dynamics (D'ortenzio et al., 2005): In winter, deep mixed layers distribute cold anomalies over a larger vertical extent, increasing thermal inertia and favoring long-lasting events. During spring and summer events, enhanced stratification confines cooling to a shallow mixed layer, leading to stronger surface anomalies and shorter MCS duration due to rapid restratification. Consistent with this behavior, the model identifies the northwest Mediterranean, eastern Tyrrhenian and Ionian Sea and parts of the Levantine basin as hotspots for long winter MCS, in line with the deep mixed layer depths of these regions during that season (Houpert et al., 2015) but in contrast to the observed hotspots of long MCS, which are found in the southern Ionian Sea.

3.2 Historical MCS in the Mediterranean Sea

3.2.1 MCS Characteristics based on MLT

To diagnose the drivers of historical MCS within the MLD we identify and examine a series of past events detected based on MLT variability. The historical MLT-based MCSs (Table S5) display similar seasonal, basin-mean properties and spatial patterns to the SST-defined events (Table S2), with spatial Pearson correlations of 0.6–0.9 and RMSE of 0.03–6 across seasons and characteristics: The basin-mean count of MLT-based MCSs peaks in autumn and reaches a minimum in winter, with hotspots identified mainly in the northern Mediterranean (Fig. S1). However, the basin-mean MCS number of the historical simulation is weakly correlated with the equivalent of the hindcast run (Fig. S1a-d), across all seasons except summer (Table S5).

MLT-based MCSs are longest in winter and shortest in summer and generally last longer than SST-based MCSs. In winter, the highest durations (~50 days) occur over the Central Mediterranean and south Aegean Sea, parts of WMED and



the Levantine basin (Fig. S2e), whereas summer MCSs are more uniformly distributed across the basin (Fig. S2g). The
275 historical simulation reproduces similar basin-mean MCS durations with the hindcast run (Fig. S2a-d), though with slightly
longer winter events and overall weak spatial agreement across seasons (Table S5).

Consistent with the SST-based MCSs (Fig. 3i-l), the intensity of MLT-based MCS is strongest in summer (-1.7°C) and
autumn (-1.6°C), with the historical simulation reproducing well the mean seasonal variability and spatial patterns relative
to the hindcast run and the observations. Both simulations identify the observed north-south gradient of high-to-low
280 intensity (Fig. 3k,l) during summer and autumn MLT-based MCSs, whereas winter and spring intensities are more uniformly
distributed across the basin (Fig. S3e-h).

Overall, the historical simulation qualitatively captures the seasonal variability and basin-mean characteristics of MLT-
based MCS: Their frequency peaks in autumn, reaches a minimum in winter when the longest events occur, whereas summer
MCSs are shorter, more intense and more uniformly distributed across the basin. The qualitative similarities with surface
285 MCS properties likely reflect the close correspondence between MLT and SST when the mixed layer is vertically
homogeneous. However, the slight quantitative differences between the basin-mean characteristics of the surface and MLT-
based MCSs likely occur when the mixed layer depth reaches its lower threshold of 10 m. In those cases, due to significant
stratification within the mixed layer, the SST is consistently warmer than the MLT. Therefore, MLT-based events tend to
have slightly longer duration but lower mean intensity than SST-based events, due to greater thermal inertia. Nevertheless,
290 the total MCS count did not show substantial differences, as expected given that MCSs are identified using percentile-based
thresholds and SST and MLT variabilities are comparable. This supports the use of the model in investigating MCS drivers
in the past and the future

For the most part of the basin, the seasonal characteristics of MLT-based MCS identified here likely reflect the
seasonality of Mediterranean MLD (Fig. S5a-d), supporting the findings by Sun et al. (2024), who reports that cold
295 anomalies in the ocean are sustained over extended periods due to a MCS-induced MLD deepening and an influence from
the mesoscale cyclonic eddies. In addition, the north-south gradient of MCS intensity simulated by both runs likely reflects
the stronger cooling and enhanced SST variability in northern Mediterranean sub-basins (e.g., Gulf of Lions, Adriatic Sea,
Aegean Sea), due to strong winds which can generate larger departures from the local climatological thresholds, compared to
the more stratified and warmer southern/eastern Mediterranean waters (e.g. Pastor et al., 2019, Pisano et al., 2020).

300

3.2.2 Drivers of MCS based on MLT

Here we assess at each grid point the frequency of each process dominating MLT-based MCSs in the historical simulation
(see Eq. 3). Figure 4 reveals a predominant influence of Forcing across all seasons, except winter. On average, 43% of the
basin's winter MCSs and particularly in the open waters of WMED, CMED and the Levantine basin develop due to strong
305 cooling induced by Forcing (Fig. 4a), whereas 52% of these events are primarily driven by Advection (Fig. 4b). Mixing
dominates locally 30-60% of winter MCSs in the northeast Levantine basin and northeast Aegean (Fig. 4c). Spring MCSs are



predominantly driven by Forcing (>70%) across the entire basin, with Advection driving 30-70% of the events in the Alboran Sea, along the southern Mediterranean and western Adriatic Sea coasts and in the northern Aegean Sea (Fig. 4d,e).

The majority (60-100%) of open-ocean summer MCSs in the WMED, CMED and southeast Levantine basin are also driven by Forcing, whereas Advection drives more than 60% of the events along the basin's coasts (Fig. 4g,h). Mixing dominates 30-70% of local summer MCS in the central and eastern Aegean, the northwest Mediterranean and the Tyrrhenian Sea and in the Gulf of Sirte (Fig. 4i). Autumn MCSs display a similar spatial distribution of dominant drivers except Mixing-driven events, which occur less frequently (<40%) across the basin (Fig. 4j-l). The seasonal distribution of historical MCS drivers closely matches that simulated by the CNRM-RCSM6 hindcast run (1982–2017), with only slight changes in the frequencies locally (Fig. S4).

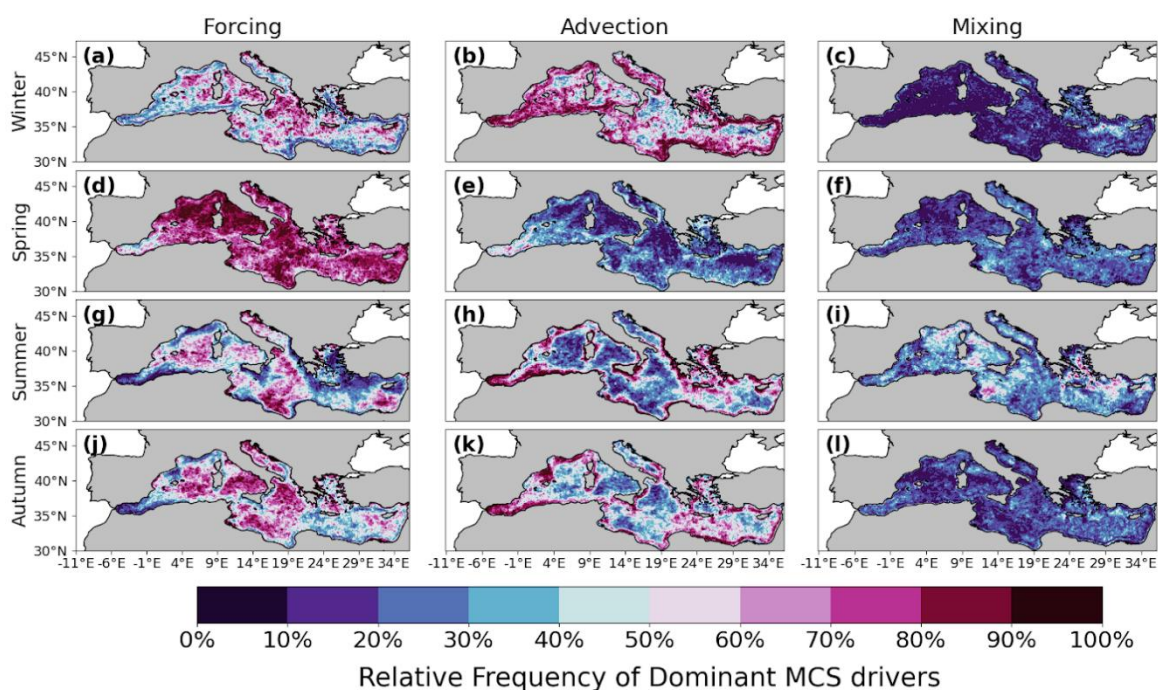


Figure 4. Seasonality of dominant drivers of historical MCSs in the Mediterranean Sea. Panels show the frequency of each MLHB process (columns) dominating the development phase of MCSs by season (rows). MCS identification was based on MLT from the CNRM-RCSM6 historical simulation (1982–2014) and climatology period of 1982-2014. At each grid point, percentage represents the number of MCS onsets attributed to each process, relative to the total number of identified onsets during the examined period. Seasonal classification is based on the date of MCS onset, with no considerations about the termination season.

A closer look at the atmospheric forcing shows that MCSs are generally associated with lower than normal surface air temperatures and higher than normal wind speeds across all seasons (Fig. S5i–l,e–h). The majority of MCSs across the basin



335 seem to co-occur with deeper than normal MLD basin-wide, except in winter and autumn, where MCSs in the northwestern Mediterranean, the CMED and the Levantine basin coincide with shallower than normal MLD (Fig. S5a,d). In particular, winter and spring MCSs in the Gulf of Lions are associated with lower than average MLD and higher than average wind speed, whereas in the Rhodes Gyre region spring MCSs seem to emerge due to the opposite conditions. Finally, summer and autumn MCSs are typically associated with higher than normal sea level pressure basin-wide (Fig. S5o,p), while during winter and spring events, most of the basin experiences lower than normal sea level pressure. However, the MCSs of those seasons in the Levantine basin are, on average, linked to higher than normal sea level pressure conditions (Fig. S5m,n).

340 The results of our analysis are consistent with previous research linking extreme cold ocean temperatures during winter to intense atmospheric cooling in the Adriatic and Ionian Sea and WMED, given the high number of atmosphere-driven events simulated in these regions during that season (e.g., Raicich et al., 2013; Chiggiato et al., 2016b; Menna et al., 2023). However, Advection emerges as the predominant driver of MCS onsets in open water during winter but affects primarily coastal areas in summer and autumn, reflecting the influence of horizontal temperature gradients and Mediterranean alongshore currents (Skloris et al., 2012). The role of mixing becomes more pronounced during summer MCS, in regions
345 where wind-induced mixing can generate and sustain surface ocean cooling (e.g Bakun et Agostini, 2001; Lebeaupin et Drobinski, 2009; Small et al., 2012; Ciappa, 2019).

3.3 Future MCS characteristics and drivers

This section focuses on projected changes in MCS characteristics and underlying mechanisms in periods of the future
350 that correspond to increasing GWLs (GWL1–GWL4), relative to both a fixed baseline in the past (1982–2014) and a moving baseline centered on each GWL (Table S1). This is, to our knowledge, the first time that these events, their characteristics, evolution and seasonal drivers in the Mediterranean Sea are systematically assessed using a daily online MLHB from a RCSM and under the SSP5-8.5 scenario. We find that projected MCS behavior depends on the chosen baseline. Our results are further discussed in the context of global MCS studies.

355 3.3.1 Future MCS characteristics based on a fixed climatology

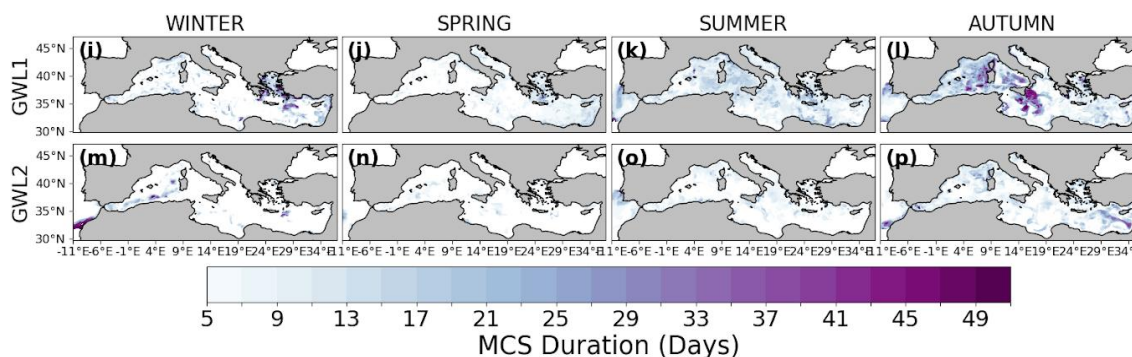
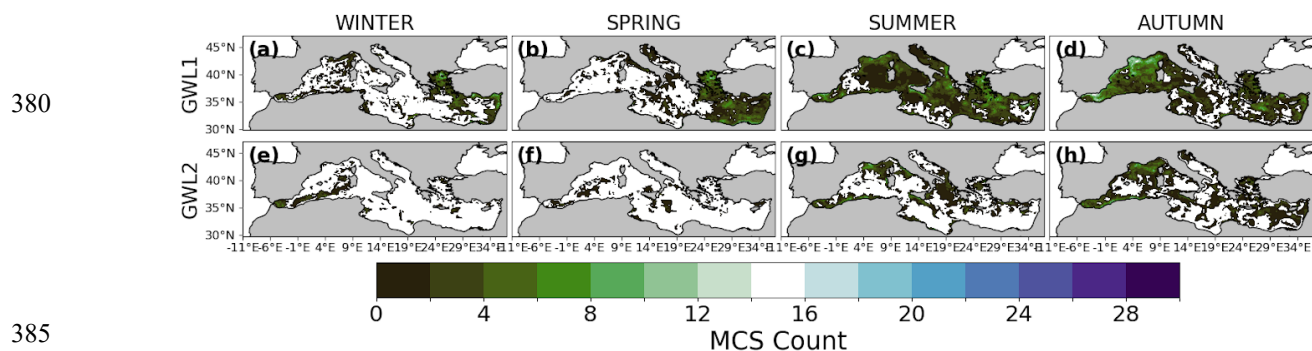
The properties of future MCS identified relative to a fixed historical climatology become weaker with increasing GWLs and display seasonal variability. Compared to historical events, MCS occurrence is projected to decline in GWL1, with the largest decrease in spring (–87 %). MCSs are also expected to become shorter, with event durations decreasing by 16 % in summer and 25 % in autumn. During these seasons, MCSs are projected to occur over a large part of the basin in GWL1
360 (Fig. 5a–d), but will be progressively limited to the northern Mediterranean and the Alboran Sea by GWL2 (Fig. 5e–h). Summer and autumn MCSs exhibit slightly higher basin-mean counts (2–3 events; Table S6) compared to winter and spring (1.2–1.4 events; Table S6). But the projected basin-mean duration is longer in autumn and winter (10–13 days; Table S6) than in spring and summer (7–10 days; Table S6; Fig. 5i–l), with future hotspots of prolonged MCSs (~ 50 days) emerging in autumn over the western Ionian Sea, the Tyrrhenian Sea, and localized regions of the western Mediterranean.



365 The regions that will remain affected by MCSs display also slightly higher basin-mean intensities in summer and autumn (-1.5 °C to -1.9 °C; Table S6; Fig. 5s,t,w,x) relative to winter and spring events (-1.2 °C up to -1.4 °C; Fig.5q,r,u,v) under GWL1. This difference may partly reflect the lower number of events and locations affected during the latter two seasons. When compared to historical events, on average, MCSs in GWL1 are projected to be -6 % less intense in the summer and -2 % in autumn.

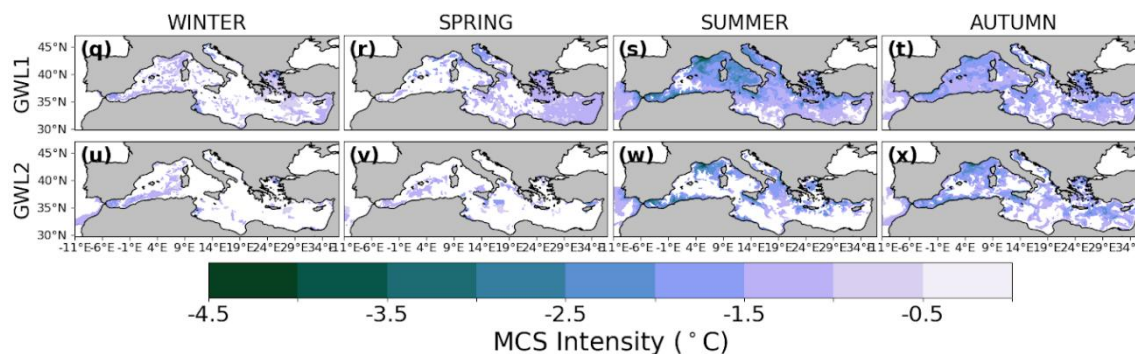
370 By GWL2 and relative to the historical period, MCSs will practically disappear from the basin, particularly in winter (-89 %) and spring (-92 %; Fig. 5a,b,e,f), with the projected reduction in summer and autumn MCS occurrence ranging from -87 % to -88 %, respectively. MCS duration and intensity are also expected to decrease by up to 50 % and 19 % ,respectively, across seasons.

375 By the mid- (GWL3) and end of the 21st century (GWL4), MCSs are absent across the entire basin and all seasons (Fig. S6e–h), with summer and autumn events under GWL3 limited to a few locations in the northern Mediterranean (Fig. S6c,d,k,l,s,t). Consequently, the following analysis of future MCS drivers focuses on GWL1 and GWL2 periods.





390



395

Figure 5: Seasonal distribution of projected MCS count (a-h), duration (i-p) and intensity (q-x) averaged over GWL1 and GWL2. Columns correspond to winter (DJF), spring (MAM), summer (JJA), and autumn (SON) events and rows to GWL1 (2007–2026) and GWL2 (2036–2055). MCSs are identified by applying the Hobday et al. (2016) framework to simulated daily MLT under SSP5-8.5, with 1982–2014 period as the baseline climatology. Seasonal classification is based on the date of MCS onset, regardless of termination. White areas indicate regions where MCS are not projected due to thermal exceedance preventing their occurrence. Equivalent results for GWL3 and GWL4 are shown in Figure S6.

400

The projected characteristics of future Mediterranean MCSs are consistent with the global reduction in MCS occurrence associated with the long-term warming of the global ocean (Yao et al., 2020, Wang et al., 2022) and the regional decline of cold extremes observed across the basin by Simon et al. (2022) and Ciappa, (2022) due to ongoing climate change. Notably, the Gulf of Lions region shows a substantial decrease in MCS occurrence by GWL1 relative to the historical period, together with a modest reduction in duration and an almost complete suppression of events by GWL2 and particularly in winter and spring. This agrees with the multi-model study by Soto-Navarro et al. (2020), who indicates a weakening of DWF in the region under the Representative Concentration Pathway (RCP) climate change scenarios.

405

3.3.2 Future MCS drivers based on a fixed climatology

410

Here, we assess changes in the frequency of future MCSs driven by Forcing (f_{for}), Advection (f_{adv}) and Mixing (f_{mix}) relative to the historical period (1982-2014). Similar to the projected MCS properties, most significant changes in MCS drivers are projected for summer and autumn events, since MCS will practically disappear progressively in winter and spring over most of the domain with higher GWLs. In particular, we find a consistent decline of the basin-mean Δf_{for} in summer and autumn events, from GWL1 (-1.5 % and -12 %) to GWL2 (-9 % and -19%) (Fig. 6c,d,g,h). However, localized Δf_{for} increases of ~50 % are projected for summer MCS in WMED and Adriatic Sea (Fig. 6c).



415 In contrast, Advection-driven MCS show a consistent basin-mean Δf_{adv} increase in autumn (12-13 %) and summer (6-14 %) events in GWL1 and GWL2 (Fig. 6k,l,o,p), Particularly in the WMED and EMED, Advection-driven MCS in autumn will locally increase by ~80% in GWL1 (Fig. 6l).

Finally, the projected response of mixing-dominated MCSs remains unclear. A variable seasonal behavior is simulated, except in the summer, when the basin-mean Δf_{mix} consistently decreases from -4.7 % in GWL1 to -5.3 % in GWL2 (Fig. 420 6s,w). However, localized increases of up to 80 % in the event frequency are projected for small areas of the central Ionian Sea and the Levantine basin in GWL1 (Fig. 6s). Overall, changes are more robust in GWL1, whereas signals in GWL2 are weaker and more spatially limited.

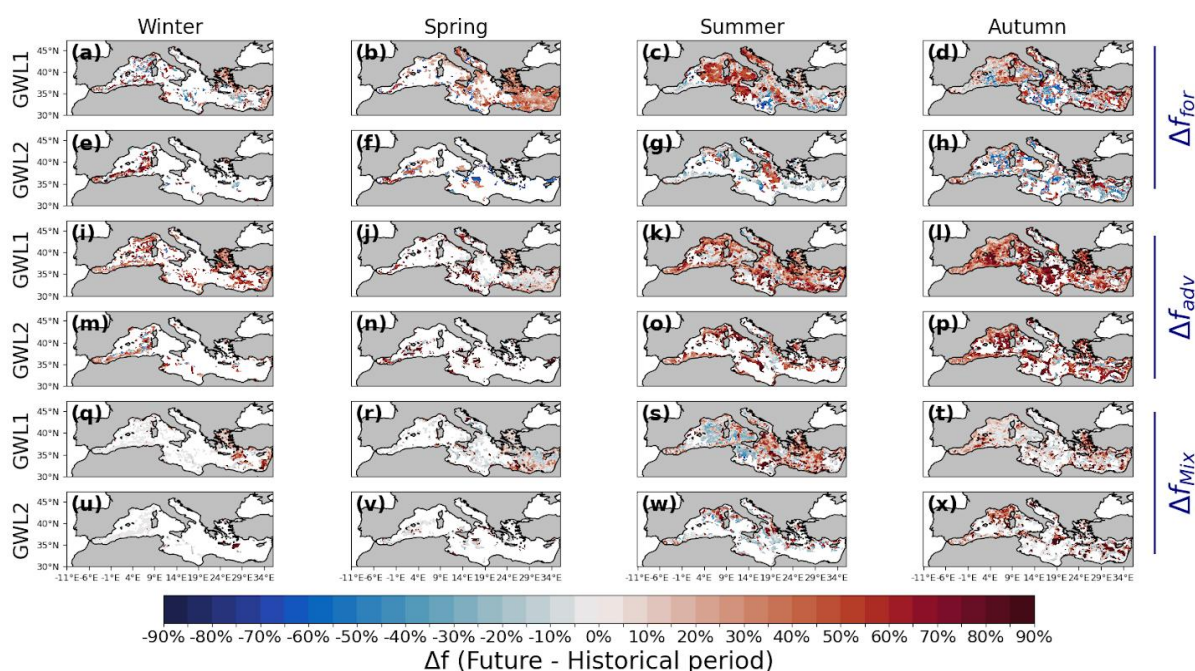
Overall, by GWL2 we find a basin-wide decline in future atmosphere-driven events, particularly in summer and autumn, while advection-driven MCSs increase consistently across most seasons, except winter. Mixing-driven MCSs show 425 heterogeneous responses. These patterns are consistent with the projections for stronger surface circulation and mesoscale activity in the basin, which increasingly modulate SST anomalies and elevate the role of dynamical ocean processes over that of surface forcing, particularly in the winter when the eddy SST signature is maximum (Ser-Giacomi et al., 2020; Parras-Berrocal et al., 2024). This is also consistent with Skliris et al. (2012), who show that decadal Mediterranean SST variability is largely driven by horizontal heat advection and increasing warming of the Atlantic inflow (Soto-Navarro et al., 430 2020) which may explain both the future disappearance of MCSs and the predominance of advection-driven mechanisms, assuming that this projected signal combines decadal internal variability with long-term climate change.

However, the limited number of MCSs in GWL1–GWL2 may bias these estimates, as rare events could overrepresent certain drivers, so the apparent decline in Forcing-driven MCSs and dominance of Advection- or Mixing-driven events during those periods should be interpreted in caution and should be confirmed with future multi-model studies.

435

440

445





450 **Figure 6:** Difference in the normalized MCS frequency between future and historical period, for events
dominated by Forcing (Δf_{for} ; a-h), Advection (Δf_{adv} ; j-p) and Mixing processes (Δf_{mix} ; q-x). Based on their date of initiation,
MCSs are grouped in winter (a,e,i,m,q,u), spring (b,f,j,n,r,y), summer (c,g,k,o,s,w) and autumn (d,h,l,p,t,x) and by warming
levels GWL1 and GWL2 (in rows). Corresponding results on GWL3 and GWL4 are not presented as MCS are too sparse
during those periods. The MCSs and their dominant drivers have been calculated relative to a fixed baseline climatology (see
455 Table S1).

3.3.3 Future MCS characteristics based on a shifted climatology

So far, future MCSs have been discussed using a fixed historical climatology of MLT as the reference period for each
season (Fig. S7) and this has shown a progressive reduction in the occurrence of most events across the basin with increasing
460 GWL (see Fig. 5 and Fig. S6). In addition, the historical MLT climatology has been previously shown to align well with the
historical SST climatology across all seasons (Darmaraki et al., 2025 in review). When MLT-based MCSs are instead
identified relative to a GWL-specific, shifted climatology in the future, they represent events occurring in the lower tail of
the future temperature distribution. Across GWL1–GWL4, this shifted baseline reflects progressively warmer mean climate
states (Fig. S8), corresponding to increasing levels of global warming relative to preindustrial conditions.

465 Here, we examine these MCSs of the future climate, which are identified against increasingly warmer climatologies (Fig.
S9) but still represent anomalously cold conditions relative to the GWL-specific mean state. For brevity, we present MCS
characteristics and their drivers in GWL2 and GWL4, as representative periods of the mid- and end of the 21st century,
respectively. Corresponding results for GWL1 and GWL3 are briefly commended and provided in the Supplementary
Material.

470 Relative to the historical period, the occurrence of future MCSs is projected to decrease in all seasons and the strongest
decrease is expected in summer MCSs with higher GWLs (from -36 % to -47 %). Despite the decline, MCSs remain more
frequent in spring than in other seasons across all GWLs (Table S7). By GWL4, the strongest reduction in MCS occurrence
is projected in the Tyrrhenian Sea, Adriatic Sea, and EMED in winter (Fig. 7e), the Liguro-Provencal and Tyrrhenian Sea,
the Gulf of Lions and Adriatic Sea in spring (Fig. 7f) and the southwestern Mediterranean and southwestern Ionian Sea in
475 the summer (Fig. 7g).

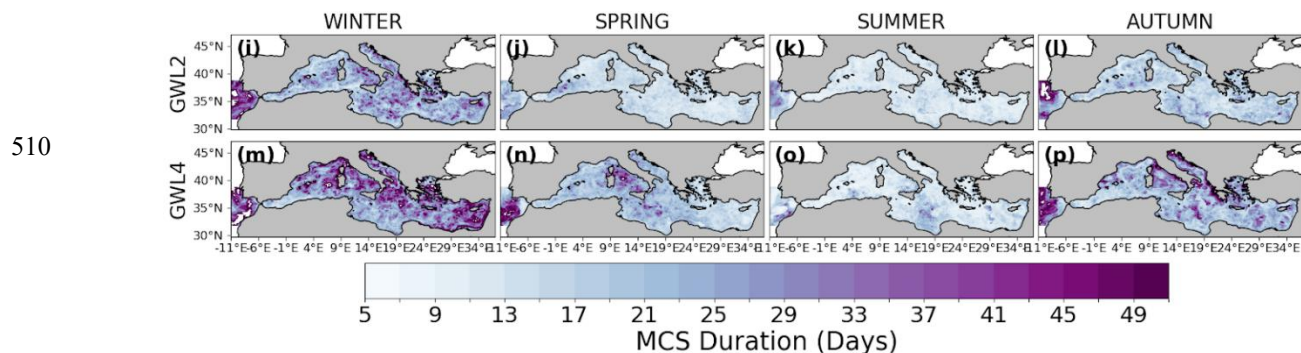
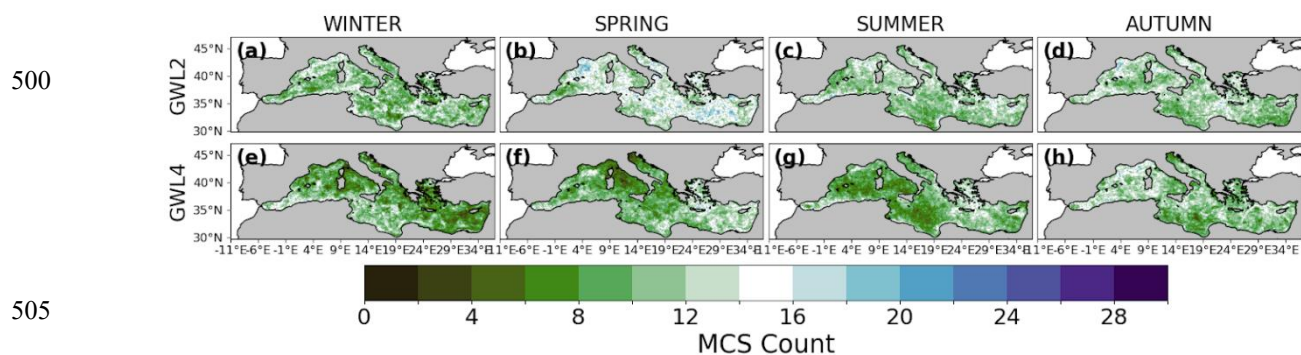
In GWL1 and GWL2, MCSs are generally shorter than the historical events by -3 % to -17 % across all seasons. By
GWL4, however, winter, spring and autumn MCSs are projected to be 9-22 % longer, whereas summer MCSs shorter by 3
% compared to historical events. From GWL2 to GWL4 basin-mean durations appear progressively longer in all seasons
except summer, with the longest durations projected in winter (21–27 days) across all GWLs (Table S7). By the end of the
480 century (GWL4), the northern Mediterranean Sea emerges as a hotspot for the longest local MCS (~ 40 days, Fig. 7m), while
comparably long spring and autumn MCS are projected over the Tyrrhenian and Adriatic Sea, respectively (Fig. 7n,p). In



GWL1 and GWL3, however, longer winter MCSs (~ 50 days) are projected over the Ionian Sea (Fig. S10i,m). Summer MCSs remain the shortest throughout all GWLs, with durations of 11–12 days, uniformly distributed across the basin (Fig. 7k,o, Table S7).

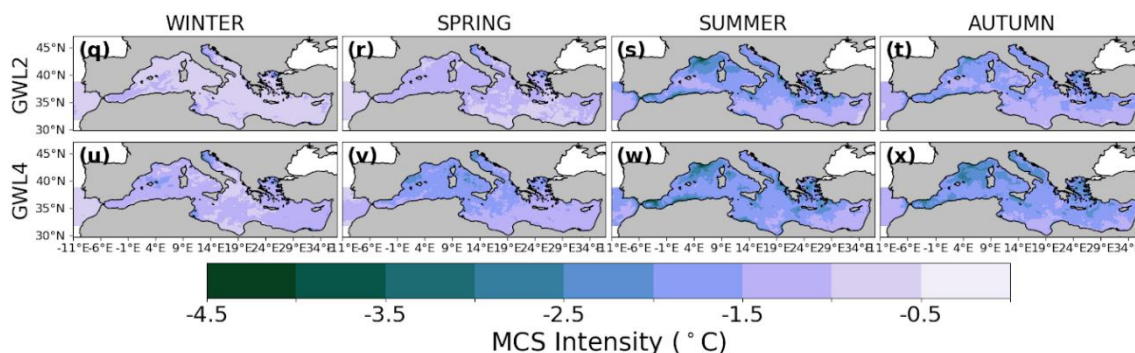
485 Finally, relative to the historical period, MCSs are projected to be -1 % to -18 % less intense in GWL1 and GWL2 across all seasons but become progressively more intense from GWL3 to GWL4. By GWL4, MCS intensity will increase by 8–16 %, with the largest intensification relative to the past occurring in spring and autumn events. The highest basin-mean intensity is projected for summer MCSs (from -1.6 °C to -1.9 °C, Table S7) and the lowest in winter MCS across all GWLs (-0.9 °C to -1.2°C, Table S7). Future summer and autumn MCSs exhibit a persistent north-to-south gradient of high to low
490 intensity from GWL2 to GWL4 (Figs. 7s,t,w,x). The persistence of the north-to-south intensity gradient in MCSs, even relative to a shifted future climatology, could indicate a north-south gradient of regional wind magnitude which may remain unchanged in the future (Parras-Berrocal et al., 2024) as well as strong atmospheric forcing. In contrast, mean winter MCS intensity is nearly uniform across the basin under both the GWL2 and GWL4 periods (Fig. 7q,u).

Overall, by GWL4 future MCSs are projected to become fewer, slightly longer and more intense compared to historical
495 events. This is in line with Chiswell, (2022), who showed higher cumulative intensities in MCSs once the climate change signal was removed. By GWL4, the longest and more intense MCSs are projected to occur in the northern Mediterranean and the eastern Levantine Basin during winter.





520



525

Figure 7: Seasonal distribution of projected MCS count (a–h), duration (i–p), and intensity (q–x). Columns correspond to winter (DJF), spring (MAM), summer (JJA), and autumn (SON), while rows show results for GWL2 and GWL4 periods. MCSs are identified by applying the Hobday et al. (2016) framework on simulated daily MLT under the SSP5-8.5 scenario, with baseline climatologies defined for each GWL. Seasons are assigned based on the date of MCS onset. Equivalent results for GWL1 and GWL3 are shown in Fig. S10.

530

3.3.4 Future MCS drivers based on a shifted climatology

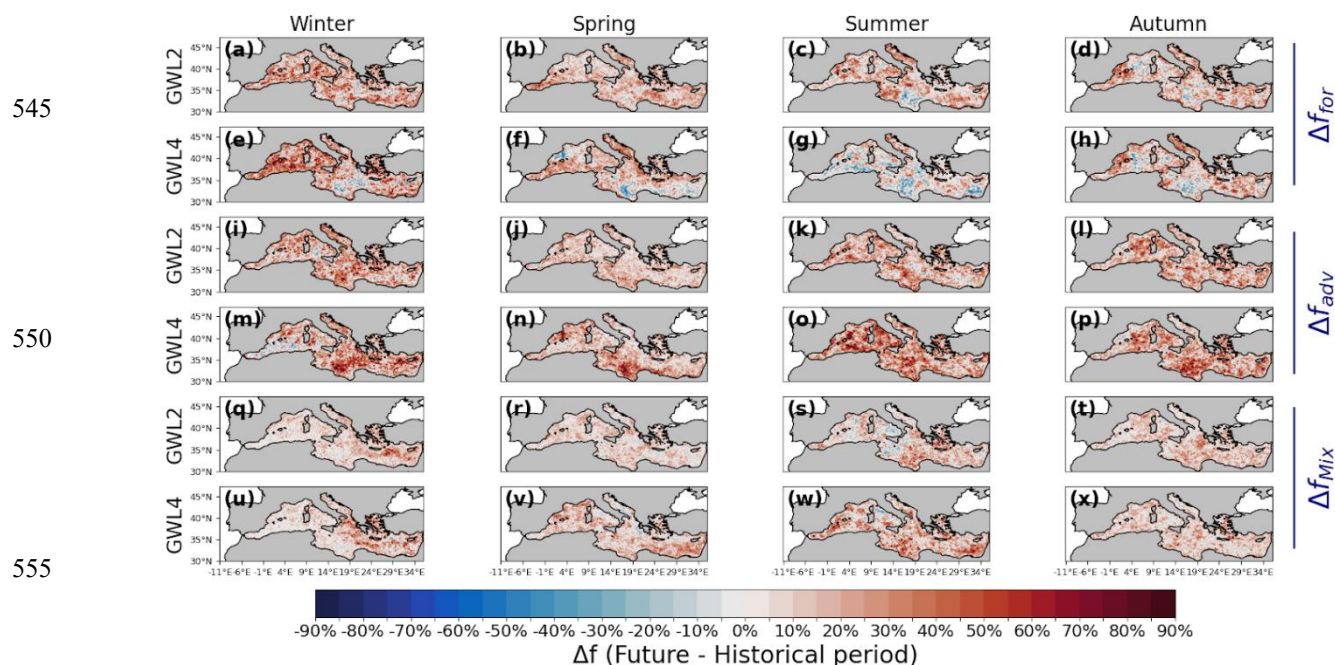
Similar to the future MCS properties described in the previous section, the relative importance of the different drivers of future MCSs varies by season and becomes more pronounced with higher GWLs. Relative to the historical period, by GWL4 the basin-mean Δf_{for} is reduced across all seasons, with the strongest decline projected in summer (-11 %; Fig. 8g) and autumn events (-1.1 % to -4 %; Fig. 8d,h & Fig. S11d,h). The latter reduction in Δf_{for} mainly affects the CMED, Algerian and southeast Levantine basin by GWL4 (Fig. 8g,h).

535

In comparison, the basin-mean Δf_{adv} increases for summer, spring and autumn events from GWL2 (~0.3 %) to GWL4 (4-8 %), with changes extending across nearly the entire basin by GWL4 (Fig. 8j-l,n-p). From GWL1 to GWL4, we also find a consistent basin-mean increasing trend in Δf_{mix} in spring and summer events (Fig. 9r,s,v,w) and a decreasing trend in winter and autumn MCSs (Fig. 9q,u,t,x).

540

Overall, the driving mechanisms of these MCSs are seasonally shifted under higher GWLs, similarly to their characteristics. The changes indicate a transition from predominantly atmospheric control of historical MCSs towards enhanced oceanic influence in future events, via vertical mixing and advection.



545

550

555

Figure 8: Difference in the MCS frequency between future f_{future} and historical period f_{hist} , for events dominated by Forcing (Δf_{for} ; a-h), Advection (Δf_{adv} ; j-p) and Mixing processes (Δf_{mix} ; q-x). Based on their date of initiation, MCSs are grouped in winter (a,e,i,m,q,u), spring (b,f,j,n,r,y), summer (c,g,k,o,s,w) and autumn (d,h,l,p,t,x) and by warming levels GWL2 and GWL4 (in rows). Corresponding results on GWL1 and GWL3 are presented in Fig. S11. The MCSs and their dominant drivers have been calculated relative to each GWL period (see Table S1).

560

565 4 Conclusion:

This study provides the first systematic assessment of characteristics and dominant drivers of Mediterranean Marine Cold Spells (MCSs) during the historical (1980-2014) period and the 21st century (2015-2100). Using the coupled regional climate system model CNRM-RCSM6 and an on-line mixed layer heat budget (MLHB) diagnostic, we identify future events under increasing global warming levels (GWLs) 1°C, 2°C, 3°C and 4°C above the pre-industrial era and the high-emission scenario SSP5-8.5. Their future properties and drivers are assessed relative to both a fixed historical period and a moving baseline centered on each GWL.

570

The CNRM-RCSM6 model reproduces well the seasonal variability (longer/shorter events during winter/summer) and basin-mean magnitude of historical surface MCSs number, duration and intensity, although spatial consistency with the observed MCS count and duration is weak. Historical MCSs are found to be more frequently driven by atmosphere forcing across all seasons, except winter, where Advection plays a dominant role across the basin, reflecting the influence of alongshore currents and mesoscale variability in dynamically active regions of the basin. Mixing plays an important role in

575



coastal and localized regions during summer and winter events, likely reflecting the effect of regional wind forcing. In addition, historical MCSs are linked with lower than normal surface air temperatures, stronger than normal wind speeds and in most cases across the basin, deeper than normal MLD.

580 When identified relative to a fixed historical baseline, future MCSs become progressively rarer, shorter and less intense and eventually nearly absent across the basin, as expected due to the mean warming of the Mediterranean Sea. Future MCSs are progressively confined to the northern areas of the Mediterranean and the Alboran Sea, with the Gulf of Lions showing a marked absence of winter MCSs by 2036-2055. The magnitude and spatial pattern of these changes, however, are sensitive to event counts and duration. By GWL3 and GWL4, MCSs occur only at a few isolated locations in the northern
585 Mediterranean, effectively disappearing from the rest of the basin across all seasons.

When MCSs are evaluated relative to a GWL-specific, shifted climatology in the future, the identified events correspond to extreme cold anomalies relative to a warmer future climate, but in absolute terms, they are warmer than historical MCSs. These "unconventional" MCSs of the future are projected to become less frequent, slightly longer and more intense by the end of the century. The simulations also project a north-south gradient of high-to low MCS intensity during summer and
590 autumn, likely associated with the stronger wind forcing in the northern parts of the basin. These future MCSs also exhibit seasonal variability, with the highest basin-mean duration projected for winter and autumn and the lowest for summer events, which are also the most intense alongside autumn MCSs. In other words, the choice of reference period against which the MCS are defined strongly affects their apparent properties in the future.

Overall, the driving mechanisms of future MCSs, whether identified relative to a fixed or to a shifted historical baseline
595 shift from a dominant atmospheric control in the historical period towards an increasing influence of vertical mixing and advection across most seasons. These findings highlight a potential reorganization of the physical drivers of Mediterranean cold extremes under climate change, with implications for upper-ocean stratification, deep water formation, thermohaline circulation and ecosystem resilience.

As the present study is based on a single future realization from one RCSM model, extending this analysis to a multi-
600 model RCSM framework is necessary to verify the robustness of our results and address their uncertainties. Understanding the evolution of MCSs is important for anticipating their impacts on productivity and deep-water ecosystems (Reale et al., 2022). Further observational validation is therefore required to reliably quantify the projected changes and assess their ecological and biogeochemical consequences. Monitoring and studying MCSs is critical for predicting climate-driven changes and informing management and policy strategies aimed at safeguarding the ecological resilience of the vulnerable
605 ecosystems of the basin.



Author contributions

Conceptualization and visualization: S.D; methodology, writing, review and editing: S.D, M.R, R.W, V.M; funding acquisition: S.D

615 Competing interests

Authors declare no competing interests.

Data Availability

620 Regional model outputs used in this study are or will be provided by the Med-CORDEX database (www.medcordex.eu/) and are available upon request

Acknowledgements

This study is part of the TexMed project, which was funded by Hellenic Foundation for Research and Innovation (H.F.R.I.) under the 3rd Call of “Research Projects to Support Post-Doctoral Researchers” scheme (Project Number 07077). M. Reale was supported by the National Recovery and Resilience Plan project TeRABIT (Terabit network for Research and Academic
625 Big data in Italy - IR0000022 - PNRR Missione 4, Componente 2, Investimento 3.1 CUP I53C21000370006) in the frame of the European Union - NextGenerationEU funding

Financial support

This study is part of the TexMed project, which was funded by Hellenic Foundation for Research and Innovation (H.F.R.I.) under the 3rd Call of “Research Projects to Support Post-Doctoral Researchers” scheme (Project Number 07077).

630 Review statement

References

Auger, P. A., Ulses, C., Estournel, C., Stemmann, L., Somot, S., and Diaz, F.: Interannual control of plankton communities by deep winter mixing and prey/predator interactions in the NW Mediterranean: Results from a 30-year 3D modeling study,
635 Progress in Oceanography, 124, 12–27, <https://doi.org/10.1016/j.pocean.2014.04.004>, 2014.



- Bakun, A. and Agostini, V. N.: Seasonal patterns of wind-induced upwelling/downwelling in the Mediterranean Sea, *Sci. mar.*, 65, 243–257, <https://doi.org/10.3989/scimar.2001.65n3243>, 2001.
- Bensi, M., Cardin, V., Rubino, A., Notarstefano, G., and Poulain, P. M.: Effects of winter convection on the deep layer of the Southern Adriatic Sea in 2012: EFFECTS OF STRONG SHELF CONVECTION, *J. Geophys. Res. Oceans*, 118, 6064–640 6075, <https://doi.org/10.1002/2013JC009432>, 2013.
- Beuvier, J., Brossier, C. L., Béranger, K., Arsouze, T., Bourdallé-Badie, R., Deltel, C., Drillet, Y., Drobinski, P., Ferry, N., Lyard, F., Sevault, F., and Somot, S.: MED12, OCEANIC COMPONENT FOR THE MODELING OF THE REGIONAL MEDITERRANEAN EARTH SYSTEM, 2012.
- Caniaux, G. and Planton, S.: A three-dimensional ocean mesoscale simulation using data from the SEMAPHORE experiment: 645 Mixed layer heat budget, *J. Geophys. Res.*, 103, 25081–25099, <https://doi.org/10.1029/98JC00452>, 1998.
- Carneiro, A. P., Soares, C. H. L., Manso, P. R. J., and Pagliosa, P. R.: Impact of marine heat waves and cold spell events on the bivalve *Anomalocardia flexuosa*: A seasonal comparison, *Marine Environmental Research*, 156, 104898, <https://doi.org/10.1016/j.marenvres.2020.104898>, 2020.
- Chiggiato, J., Schroeder, K., and Trincardi, F.: Cascading dense shelf-water during the extremely cold winter of 2012 in the 650 Adriatic, Mediterranean Sea: Formation, flow, and seafloor impact, *Marine Geology*, 375, 1–4, <https://doi.org/10.1016/j.margeo.2016.03.002>, 2016a.
- Chiggiato, J., Bergamasco, A., Borghini, M., Falcieri, F. M., Falco, P., Langone, L., Miserocchi, S., Russo, A., and Schroeder, K.: Dense-water bottom currents in the Southern Adriatic Sea in spring 2012, *Marine Geology*, 375, 134–145, <https://doi.org/10.1016/j.margeo.2015.09.005>, 2016b.
- 655 Ciappa, A. C.: The summer upwelling of the Eastern Aegean Sea detected from MODIS SST scenes from 2003 to 2015, *International Journal of Remote Sensing*, 40, 3105–3117, <https://doi.org/10.1080/01431161.2018.1539272>, 2019.
- Ciappa, A. C.: Effects of Marine Heatwaves (MHW) and Cold Spells (MCS) on the surface warming of the Mediterranean Sea from 1989 to 2018, *Progress in Oceanography*, 205, 102828, <https://doi.org/10.1016/j.pocean.2022.102828>, 2022.
- Colella, M. A., Ruzicka, R. R., Kidney, J. A., Morrison, J. M., and Brinkhuis, V. B.: Cold-water event of January 2010 results 660 in catastrophic benthic mortality on patch reefs in the Florida Keys, *Coral Reefs*, 31, 621–632, <https://doi.org/10.1007/s00338-012-0880-5>, 2012.
- Company, J. B., Puig, P., Sardà, F., Palanques, A., Latasa, M., and Scharek, R.: Climate Influence on Deep Sea Populations, *PLoS ONE*, 3, e1431, <https://doi.org/10.1371/journal.pone.0001431>, 2008.
- Darmaraki, S., Somot, S., Sevault, F., Nabat, P., Cabos Narvaez, W. D., Cavicchia, L., Djurdjevic, V., Li, L., Sannino, G., and 665 Sein, D. V.: Future evolution of Marine Heatwaves in the Mediterranean Sea, *Clim Dyn*, 53, 1371–1392, <https://doi.org/10.1007/s00382-019-04661-z>, 2019a.
- Darmaraki, S., Somot, S., Sevault, F., and Nabat, P.: Past Variability of Mediterranean Sea Marine Heatwaves, *Geophysical Research Letters*, 46, 9813–9823, <https://doi.org/10.1029/2019GL082933>, 2019b.



- Darmaraki, S., Denaxa, D., Theodorou, I., Livanou, E., Rigatou, D., E, D. R., Stavrakidis-Zachou, O., Dimarchopoulou, D.,
670 Bonino, G., McADAM, R., Organelli, E., Pitsouni, A., and Parasyris, A.: Marine Heatwaves in the Mediterranean Sea: A
Literature Review, *Mediterranean Marine Science*, 25, 586–620, <https://doi.org/10.12681/mms.38392>, 2024.
- Darmaraki, S., Waldman, R., Somot, S., and Sevault, F.: Climate Change shifts drivers of Mediterranean Marine Heatwaves,
Climate Dynamics, under review, 2025.
- D’Ortenzio, F., Iudicone, D., De Boyer Montegut, C., Testor, P., Antoine, D., Marullo, S., Santoleri, R., and Madec, G.:
675 Seasonal variability of the mixed layer depth in the Mediterranean Sea as derived from in situ profiles, *Geophysical
Research Letters*, 32, 2005GL022463, <https://doi.org/10.1029/2005GL022463>, 2005.
- Economidis, P. S. and Vogiatzis, V. P.: Mass mortality of *Sardinella aurita* Valenciennes (Pisces, Clupeidae) in Thessaloniki
Bay (Macedonia, Greece), *Journal of Fish Biology*, 41, 147–149, <https://doi.org/10.1111/j.1095-8649.1992.tb03178.x>,
1992.
- 680 Font, J., Puig, P., Salat, J., Palanques, A., and Emelianov, M.: Sequence of hydrographic changes in NW Mediterranean deep
water due to the exceptional winter of 2005, *Sci. mar.*, 71, 339–346, <https://doi.org/10.3989/scimar.2007.71n2339>, 2007.
- Gori, A., Orejas, C., Madurell, T., Bramanti, L., Martins, M., Quintanilla, E., Marti-Puig, P., Lo Iacono, C., Puig, P.,
Requena, S., Greenacre, M., and Gili, J. M.: Bathymetrical distribution and size structure of cold-water coral populations
in the Cap de Creus and Lacaze-Duthiers canyons (northwestern Mediterranean), *Biogeosciences*, 10, 2049–2060,
685 <https://doi.org/10.5194/bg-10-2049-2013>, 2013.
- Guillén, J., Arin, L., Estrada, M., Salat, J., Puig, P., Palanques, A., and Pascual, J.: Coastal hydrographic signatures of heat
waves and extreme events of dense water formation during 2002–2012 (Barcelona, NW Mediterranean), 2015.
- Gunter, G. and Hildebrand, H. H.: Destruction of Fishes and Other Organisms on the South Texas Coast by the Cold Wave of
January 28–February 3, 1951, *Ecology*, 32, 731–736, <https://doi.org/10.2307/1932740>, 1951.
- 690 Hauser, M., Engelbrecht, F., and Fischer, E. M.: Transient global warming levels for CMIP5 and CMIP6, ,
<https://doi.org/10.5281/ZENODO.7390473>, 2022.
- Hobday, A. J., Alexander, L. V., Perkins, S. E., Smale, D. A., Straub, S. C., Oliver, E. C. J., Benthuyssen, J. A., Burrows, M.
T., Donat, M. G., Feng, M., Holbrook, N. J., Moore, P. J., Scannell, H. A., Sen Gupta, A., and Wernberg, T.: A
hierarchical approach to defining marine heatwaves, *Progress in Oceanography*, 141, 227–238,
695 <https://doi.org/10.1016/j.pocean.2015.12.014>, 2016.
- Houpert, L., Testor, P., Durrieu de Madron, X., Somot, S., D’Ortenzio, F., Estournel, C., and Lavigne, H.: Seasonal cycle of
the mixed layer, the seasonal thermocline and the upper-ocean heat storage rate in the Mediterranean Sea derived from
observations, *Progress in Oceanography*, 132, 333–352, <https://doi.org/10.1016/j.pocean.2014.11.004>, 2015.
- Janeković, I., Mihanović, H., Vilibić, I., and Tudor, M.: Extreme cooling and dense water formation estimates in open and
700 coastal regions of the Adriatic Sea during the winter of 2012, *J. Geophys. Res. Oceans*, 119, 3200–3218,
<https://doi.org/10.1002/2014JC009865>, 2014.



- Jentsch, A., Kreyling, J., and Beierkuhnlein, C.: A new generation of climate-change experiments: events, not trends, *Frontiers in Ecology and the Environment*, 5, 365–374, [https://doi.org/10.1890/1540-9295\(2007\)5%255B365:ANGOCE%255D2.0.CO;2](https://doi.org/10.1890/1540-9295(2007)5%255B365:ANGOCE%255D2.0.CO;2), 2007.
- 705
- Kotta, D. and Kitsiou, D.: Chlorophyll in the Eastern Mediterranean Sea: Correlations with Environmental Factors and Trends, *Environments*, 6, 98, <https://doi.org/10.3390/environments6080098>, 2019.
- Lebeauvin Brossier, C. and Drobinski, P.: Numerical high-resolution air-sea coupling over the Gulf of Lions during two tramontane/mistral events, *J. Geophys. Res.*, 114, 2008JD011601, <https://doi.org/10.1029/2008JD011601>, 2009.
- 710 Lirman, D., Schopmeyer, S., Manzello, D., Gramer, L. J., Precht, W. F., Muller-Karger, F., Banks, K., Barnes, B., Bartels, E., Bourque, A., Byrne, J., Donahue, S., Duquesnel, J., Fisher, L., Gilliam, D., Hendee, J., Johnson, M., Maxwell, K., McDevitt, E., Monty, J., Rueda, D., Ruzicka, R., and Thanner, S.: Severe 2010 Cold-Water Event Caused Unprecedented Mortality to Corals of the Florida Reef Tract and Reversed Previous Survivorship Patterns, *PLoS ONE*, 6, e23047, <https://doi.org/10.1371/journal.pone.0023047>, 2011.
- 715 López-Jurado, J. -L., González-Pola, C., and Vélez-Belchí, P.: Observation of an abrupt disruption of the long-term warming trend at the Balearic Sea, western Mediterranean Sea, in summer 2005, *Geophysical Research Letters*, 32, 2005GL024430, <https://doi.org/10.1029/2005GL024430>, 2005.
- Madec, Gurvan. "NEMO ocean engine." (2015).
- Manna, V., Fabbro, C., Cerino, F., Bazzaro, M., Del Negro, P., and Celussi, M.: Effect of an extreme cold event on the metabolism of planktonic microbes in the northernmost basin of the Mediterranean Sea, *Estuarine, Coastal and Shelf Science*, 225, 106252, <https://doi.org/10.1016/j.ecss.2019.106252>, 2019.
- 720
- Martin, P., Maynou, F., Recasens, L., and Sabatés, A.: Cyclic fluctuations of blue whiting (*Micromesistius poutassou*) linked to open-sea convection processes in the northwestern Mediterranean, *Fisheries Oceanography*, 25, 229–240, <https://doi.org/10.1111/fog.12147>, 2016.
- 725 Menna, M., Martellucci, R., Reale, M., Cossarini, G., Salon, S., Notarstefano, G., Mauri, E., Poulain, P.-M., Gallo, A., and Solidoro, C.: A case study of impacts of an extreme weather system on the Mediterranean Sea circulation features: Mediane Apollo (2021), *Sci Rep*, 13, 3870, <https://doi.org/10.1038/s41598-023-29942-w>, 2023.
- Mihanović, H., Vilibić, I., Carniel, S., Tudor, M., Russo, A., Bergamasco, A., Bubić, N., Ljubešić, Z., Viličić, D., Boldrin, A., Malačić, V., Celio, M., Comici, C., and Raicich, F.: Exceptional dense water formation on the Adriatic shelf in the winter
- 730 of 2012, *Ocean Sci.*, 9, 561–572, <https://doi.org/10.5194/os-9-561-2013>, 2013.
- Orejas, C., Gori, A., Lo Iacono, C., Puig, P., Gili, J., and Dale, M.: Cold-water corals in the Cap de Creus canyon, northwestern Mediterranean: spatial distribution, density and anthropogenic impact, *Mar. Ecol. Prog. Ser.*, 397, 37–51, <https://doi.org/10.3354/meps08314>, 2009.
- Parras-Berrocal, I. M., Waldman, R., Sevault, F., Somot, S., Gonzalez, N., Ahrens, B., Anav, A., Djurdjević, V., Gualdi, S.,
- 735 Hamouda, M. E., Li, L., Lionello, P., Sannino, G., and Sein, D. V.: Response of the Mediterranean Sea Surface Circulation



- at Various Global Warming Levels: A Multi-Model Approach, *Geophysical Research Letters*, 51, e2024GL111695, <https://doi.org/10.1029/2024GL111695>, 2024.
- Parras-Berrocal, I. M., Waldman, R., Gonzalez, N. M., Ahrens, B., Cabos, W., Jordà, G., Lionello, P., Sannino, G., and Somot, S.: Regionalized Mediterranean relative sea level projections under high-emission regional climate scenarios, *Environ. Res. Lett.*, 20, 114068, <https://doi.org/10.1088/1748-9326/ae15a5>, 2025.
- Pastor, F., Valiente, J. A., and Palau, J. L.: Sea Surface Temperature in the Mediterranean: Trends and Spatial Patterns (1982–2016), in: *Meteorology and Climatology of the Mediterranean and Black Seas*, edited by: Vilibić, I., Horvath, K., and Palau, J. L., Springer International Publishing, Cham, 297–309, https://doi.org/10.1007/978-3-030-11958-4_18, 2019.
- 745 Penzar, B., Penzar, I., and Orlić, M.: Weather and Climate of the Croatian Adriatic (in Croatian), *Nakladna kuća “Dr. Feletar”*, Hydrographic Institute of the Republic of Croatia, Split, 258 pp., 2001
- Petrelli, P.: XMHW: Xarray based code to identify Marine HeatWave events and their characteristics, , <https://doi.org/10.5281/ZENODO.6270280>, 2022.
- 750 Pilo, G. S., Holbrook, N. J., Kiss, A. E., and Hogg, A. McC.: Sensitivity of Marine Heatwave Metrics to Ocean Model Resolution, *Geophysical Research Letters*, 46, 14604–14612, <https://doi.org/10.1029/2019GL084928>, 2019.
- Pisano, A., Buongiorno Nardelli, B., Tronconi, C., and Santoleri, R.: The new Mediterranean optimally interpolated pathfinder AVHRR SST Dataset (1982–2012), *Remote Sensing of Environment*, 176, 107–116, <https://doi.org/10.1016/j.rse.2016.01.019>, 2016.
- 755 Pisano, A., Marullo, S., Artale, V., Falcini, F., Yang, C., Leonelli, F. E., Santoleri, R., and Buongiorno Nardelli, B.: New Evidence of Mediterranean Climate Change and Variability from Sea Surface Temperature Observations, *Remote Sensing*, 12, 132, <https://doi.org/10.3390/rs12010132>, 2020.
- Querin, S., Bensi, M., Cardin, V., Solidoro, C., Bacer, S., Mariotti, L., Stel, F., and Malačić, V.: Saw-tooth modulation of the deep-water thermohaline properties in the southern Adriatic Sea, *JGR Oceans*, 121, 4585–4600, <https://doi.org/10.1002/2015JC011522>, 2016.
- 760 Raicich, F., Malačić, V., Celio, M., Gaiotti, D., Cantoni, C., Colucci, R. R., Čermelj, B., and Pucillo, A.: Extreme air-sea interactions in the Gulf of Trieste (North Adriatic) during the strong Bora event in winter 2012: AIR-SEA INTERACTIONS IN WINTER 2012, *J. Geophys. Res. Oceans*, 118, 5238–5250, <https://doi.org/10.1002/jgrc.20398>, 2013.
- 765 Reale, M., Cossarini, G., Lazzari, P., Lovato, T., Bolzon, G., Masina, S., Solidoro, C., and Salon, S.: Acidification, deoxygenation, and nutrient and biomass declines in a warming Mediterranean Sea, *Biogeosciences*, 19, 4035–4065, <https://doi.org/10.5194/bg-19-4035-2022>, 2022.
- Rohling, E. J., Hayes, A., De Rijk, S., Kroon, D., Zachariasse, W. J., and Eisma, D.: Abrupt cold spells in the northwest Mediterranean, *Paleoceanography*, 13, 316–322, <https://doi.org/10.1029/98PA00671>, 1998.



- 770 Ruti, P. M., Somot, S., Giorgi, F., Dubois, C., Flaounas, E., Obermann, A., Dell’Aquila, A., Pisacane, G., Harzallah, A., Lombardi, E., Ahrens, B., Akhtar, N., Alias, A., Arsouze, T., Aznar, R., Bastin, S., Bartholy, J., Béranger, K., Beuvier, J., Bouffies-Cloch e, S., Brauch, J., Cabos, W., Calmanti, S., Calvet, J.-C., Carillo, A., Conte, D., Coppola, E., Djurdjevic, V., Drobinski, P., Elizalde-Arellano, A., Gaertner, M., Gal n, P., Gallardo, C., Gualdi, S., Goncalves, M., Jorba, O., Jord , G., L’Heveder, B., Lebeaupin-Brossier, C., Li, L., Liguori, G., Lionello, P., Maci s, D., Nabat, P.,  nol, B., Raikovic, B.,
- 775 Ramage, K., Sevault, F., Sannino, G., Struglia, M. V., Sanna, A., Torma, C., and Vervatis, V.: Med-CORDEX Initiative for Mediterranean Climate Studies, *Bulletin of the American Meteorological Society*, 97, 1187–1208, <https://doi.org/10.1175/BAMS-D-14-00176.1>, 2016.
- Salat, J. and Pascual Massaguer, J.: Principales tendencias climatol gicas en el mediterr neo noroccidental, a partir de m s de 30 a os de observaciones oceanogr ficas y meteorol gicas en la costa catalana, *Asociaci n Espa ola de Climatolog a*, 780 2006.
- Schlegel, R. W., Oliver, E. C. J., Wernberg, T., and Smit, A. J.: Nearshore and offshore co-occurrence of marine heatwaves and cold-spells, *Progress in Oceanography*, 151, 189–205, <https://doi.org/10.1016/j.pocean.2017.01.004>, 2017.
- Schlegel, R. W., Darmaraki, S., Benthuisen, J. A., Filbee-Dexter, K., and Oliver, E. C. J.: Marine cold-spells, *Progress in Oceanography*, 198, 102684, <https://doi.org/10.1016/j.pocean.2021.102684>, 2021.
- 785 Schroeder, K., Ribotti, A., Borghini, M., Sorgente, R., Perilli, A., and Gasparini, G. P.: An extensive western Mediterranean deep water renewal between 2004 and 2006, *Geophysical Research Letters*, 35, 2008GL035146, <https://doi.org/10.1029/2008GL035146>, 2008.
- Ser-Giacomi, E., Jord -S nchez, G., Soto-Navarro, J., Thomsen, S., Mignot, J., Sevault, F., and Rossi, V.: Impact of Climate Change on Surface Stirring and Transport in the Mediterranean Sea, *Geophysical Research Letters*, 47, e2020GL089941, 790 <https://doi.org/10.1029/2020GL089941>, 2020.
- Sevault, F.: Atlas of the 1980-2018 ERA-Interim simulation with the coupled regional climate system model CNRM-RCSM6, <https://doi.org/10.5281/ZENODO.11066601>, 2024.
- Sevault, F., Somot, S., Alias, A., Dubois, C., Lebeaupin-Brossier, C., Nabat, P., Adloff, F., D qu , M., and Decharme, B.: A fully coupled Mediterranean regional climate system model: design and evaluation of the ocean component for the 1980– 795 2012 period, *Tellus A: Dynamic Meteorology and Oceanography*, 66, 23967, <https://doi.org/10.3402/tellusa.v66.23967>, 2014.
- Simon, A., Plecha, S. M., Russo, A., Teles-Machado, A., Donat, M. G., Auger, P.-A., and Trigo, R. M.: Hot and cold marine extreme events in the Mediterranean over the period 1982-2021, *Front. Mar. Sci.*, 9, <https://doi.org/10.3389/fmars.2022.892201>, 2022.
- 800 Skliris, N., Sofianos, S., Gkanasos, A., Mantziafou, A., Vervatis, V., Axaopoulos, P., and Lascaratos, A.: Decadal scale variability of sea surface temperature in the Mediterranean Sea in relation to atmospheric variability, *Ocean Dynamics*, 62, 13–30, <https://doi.org/10.1007/s10236-011-0493-5>, 2012.



- Small, R. J., Carniel, S., Campbell, T., Teixeira, J., and Allard, R.: The response of the Ligurian and Tyrrhenian Seas to a summer Mistral event: A coupled atmosphere–ocean approach, *Ocean Modelling*, 48, 30–44, 805 <https://doi.org/10.1016/j.ocemod.2012.02.003>, 2012.
- Somot, S., Ruti, P., Ahrens, B., Coppola, E., Jordà, G., Sannino, G., and Solmon, F.: Editorial for the Med-CORDEX special issue, *Clim Dyn*, 51, 771–777, <https://doi.org/10.1007/s00382-018-4325-x>, 2018.
- Soto-Navarro, J., Jordà, G., Amores, A., Cabos, W., Somot, S., Sevault, F., Macías, D., Djurdjevic, V., Sannino, G., Li, L., and Sein, D.: Evolution of Mediterranean Sea water properties under climate change scenarios in the Med-CORDEX ensemble, *Clim Dyn*, 54, 2135–2165, <https://doi.org/10.1007/s00382-019-05105-4>, 2020. 810
- Sun, D., Liu, Z., Chiu, L., Yang, R., Singh, R. P., and Kafatos, M.: Anomalous cold water detected along Mid-Atlantic Coast, *EoS Transactions*, 85, 152–152, <https://doi.org/10.1029/2004EO150003>, 2004.
- Sun, W., Wang, Y., Yang, Y., Yang, J., Ji, J., and Dong, C.: Marine Heatwaves/Cold-Spells Associated With Mixed Layer Depth Variation Globally, *Geophysical Research Letters*, 51, e2024GL112325, <https://doi.org/10.1029/2024GL112325>, 815 2024.
- Taviani, M., Angeletti, L., Beuck, L., Campiani, E., Canese, S., Foglini, F., Freiwald, A., Montagna, P., and Trincardi, F.: Reprint of “On and off the beaten track: Megafaunal sessile life and Adriatic cascading processes,” *Marine Geology*, 375, 146–160, <https://doi.org/10.1016/j.margeo.2015.10.003>, 2016.
- Teruzzi, A., Aydogdu, A., Amadio, C., Clementi, E., Colella, S., Di Biagio, V., Drudi, M., Fanelli, C., Feudale, L., Grandi, A., Miraglio, P., Pisano, A., Pistoia, J., Reale, M., Salon, S., Volpe, G., and Cossarini, G.: Anomalous 2022 deep-water 820 formation and intense phytoplankton bloom in the Cretan area, *State of the Planet*, 4-osr8, 1–15, <https://doi.org/10.5194/sp-4-osr8-15-2024>, 2024.
- Tréguier, A. M., De Boyer Montégut, C., Chassignet, E., Fox-Kemper, B., Hogg, A., Iovino, D., Kiss, A., Le Sommer, J., Lique, C., Lin, P., Liu, H., Serazin, G., Sidorenko, D., Yeager, S., and Wang, Q.: The mixed layer depth in Ocean Model Intercomparison Project (OMIP) high resolution models, <https://doi.org/10.5194/egusphere-egu23-8162>, 825
- Tsimplis, M. N., Marcos, M., and Somot, S.: 21st century Mediterranean sea level rise: Steric and atmospheric pressure contributions from a regional model, *Global and Planetary Change*, 63, 105–111, <https://doi.org/10.1016/j.gloplacha.2007.09.006>, 2008.
- Velaoras, D., Papadopoulos, V. P., Kontoyiannis, H., Papageorgiou, D. K., and Pavlidou, A.: The Response of the Aegean 830 Sea (Eastern Mediterranean) to the Extreme 2016–2017 Winter, *Geophysical Research Letters*, 44, 9416–9423, <https://doi.org/10.1002/2017GL074761>, 2017.
- Wang, Y., Kajtar, J. B., Alexander, L. V., Pilo, G. S., and Holbrook, N. J.: Understanding the Changing Nature of Marine Cold-Spells, *Geophysical Research Letters*, 49, e2021GL097002, <https://doi.org/10.1029/2021GL097002>, 2022.
- 835 Yao, Y., Wang, C., and Fu, Y.: Global Marine Heatwaves and Cold-Spells in Present Climate to Future Projections, *Earth’s Future*, 10, e2022EF002787, <https://doi.org/10.1029/2022EF002787>, 2022.